

Electrochemical Performance of Mn Doped Co_3O_4 Supercapacitor: Effect of Aqueous Electrolytes

Jogade SM* and Sutrave DS

Department of Electronics, D.B.F Dayanand College of Arts and Science, Solapur, MS, India

Abstract

Effect of aqueous electrolytes (KOH, KCl, CH_3COONa and NH_4Cl) on electrochemical behaviour of Supercapacitor was studied by cyclic voltammetry, cyclic stability, and electrochemical impedance analysis. The results show that among all aqueous electrolytes investigated, KOH revealed good supercapacitive behaviour and exhibited 675Fgm^{-1} specific capacitance, 86% of cyclic stability, 100% columbic efficiency and 8Ω equivalent series resistance ESR.

Keywords: Aqueous electrolytes; KOH; CV; EIS; Specific capacitance; Stability; ESR

Introduction

Supercapacitors, also known as ultracapacitors, electric double layer capacitors (EDLCs) or electrochemical supercapacitors are the electrochemical energy storage devices in which the electric charge is stored in the electrical double layer formed at the interface between electrode and an electrolyte solution. These devices can provide high power capability, excellent reversibility and long cycle life [1-3]. Even though super capacitors are now commercially available, they still require improvements, especially for enhancing their power density and cut the cost at the same time. To reach these objectives, various strategies have been proposed in the literature, involving the development of new materials, new geometries and electrolytes [4].

The electrolyte is the key part of the electrochemical capacitors as the operating voltage, specific capacitance, power density are greatly influenced by the choice of electrolyte. Literature study also indicate that the factors affecting the energy storage capacity of super capacitor are particle size and electrochemical conditions, namely type of electrolyte, concentration of electrolyte, conductivity of the electrolyte, scan rate, etc. [5-9]. Therefore, the electrolytic system must exhibit, a good conductance which determines the power output capability and a good ionic adsorption which determines the specific double-layer capacitance. Overall, the desirable properties of an electrolytic system for super capacitors are high ionic conductivity, wide voltage window, and high electrochemical and thermal stability, low viscosity, low toxicity, low cost, etc. [10]. Compared with non-aqueous electrolytes, the aqueous medium provides a much higher conductivity leading to higher power density. On the other hand, low cost and easy manipulation could be further advantages for aqueous electrolytes.

Until recently, the most commonly used aqueous electrolytes were H_2SO_4 and KOH [11]. Hence in the present work attempts are made to study various electrochemical properties of supercapacitor with different aqueous electrolytes such as KOH, KCl, CH_3COONa and NH_4Cl by implementing cyclic voltammetry (CV) and electrochemical impedance spectroscopy (EIS).

Experimental Section

The supercapacitor cell under test is made up of 1% Manganese doped Cobalt oxide thin film as its working electrode, platinum wire as counter electrode and saturated calomel (SCE) as reference electrode and aqueous electrolyte. The various electrochemical properties of supercapacitor were tested with different aqueous electrolytes such as

KOH, KCl, CH_3COONa and NH_4Cl each of 0.1 M concentration. Thin film electrodes were fabricated by using Sol-gel spin coat deposition technique using stainless steel as substrate. The detailed synthesis and deposition process is discussed in the earlier paper [12].

All characterizations done with the help of CHI608E Electrochemical Workstation. Electrochemical impedance analysis was done by using ZSimpWin Simulation software.

Result and Discussion

Structural properties

The structural analysis of the deposited thin film was done by using X-ray diffractometer varying diffraction angle 2θ from 10° to 90° . Figure 1 shows the X-ray diffraction pattern (XRD) of 1% Mn doped Cobalt oxide thin film. XRD pattern exhibited high intensity diffraction peaks cubic Co_3O_4 and orthorhombic MnO_2 phase. Which indicates film is crystalline in nature. The XRD data were matched with JCPDS card 78-1969 and 82-2169 for cobalt and manganese peaks respectively.

Morphological properties

Figure 2 shows the SEM micrographs of Mn-doped Co_3O_4 films on the stainless steel substrate at two different magnifications $\times 10,000$ and $\times 40,000$. SEM images showed the formation of many tetragonal particles spread smoothly all over the substrate surface. At higher magnification ($\times 40,000$), it can be clearly observed that the grains are internally connected with each other and provide porous surface morphology. Average grain size was calculated from the SEM micrographs and it was approximately $0.22\ \mu\text{m}$.

Electrochemical analysis

Cyclic voltammetry: Figure 3 shows the cyclic voltammetry curves for different aqueous electrolytes KOH, KCl, NH_4Cl and CH_3COONa . Scan rate is varied from 10 to 100 mV/s. It has been observed from the

*Corresponding author: Jogade SM, Department of Electronics, D.B.F Dayanand College of Arts and Science, Solapur, MS, India; Tel: 0217 232 3193; E-mail: m5jogade@gmail.com

Received June 16, 2017; Accepted June 28, 2017; Published June 31, 2017

Citation: Jogade SM, Sutrave DS (2017) Electrochemical Performance of Mn Doped Co_3O_4 Supercapacitor: Effect of Aqueous Electrolytes. J Material Sci Eng 6: 351. doi: 10.4172/2169-0022.1000351

Copyright: © 2017 Jogade SM, et al. This is an open-access article distributed under the terms of the Creative Commons Attribution License, which permits unrestricted use, distribution, and reproduction in any medium, provided the original author and source are credited.

figures that the optimized potential window and the current density are different for all electrolytes.

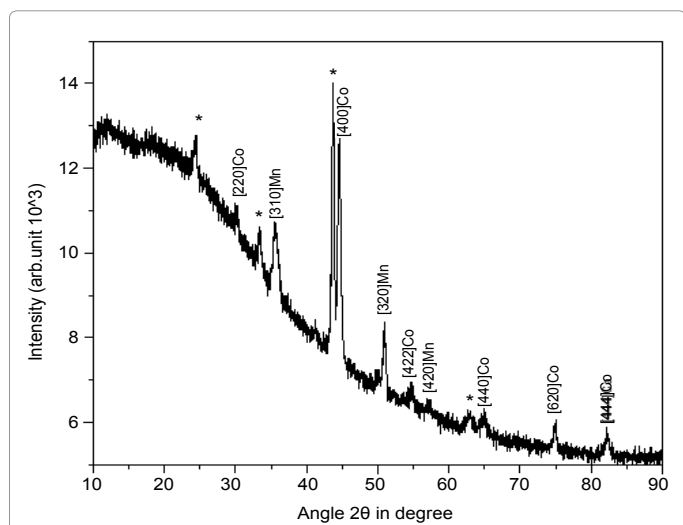


Figure 1: XRD pattern of spin coat deposited 1% Mn doped Cobalt oxide thin film.

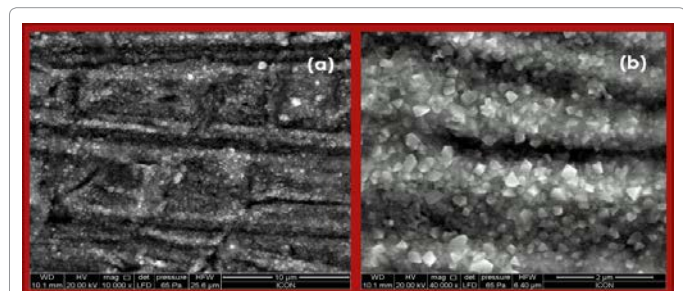


Figure 2: SEM micrographs of spin coat deposited 1% Mn doped Cobalt oxide thin film.

CV Curves for all the electrolytes exhibited a common trend of decreasing specific capacitance values against an increasing scan rate. It is because for very low scan rates the ions have a much longer time to penetrate and reside in the electrode pores and form electric double layers, leading to increase in specific capacitance.

A rectangular type of voltammogram is the indication of ideal capacitive behaviour of any material [13]. But CV curves of KOH and KCl electrolyte showed redox transition peaks at prescribed potentials. This indicates that, the supercapacitive characteristics are mainly governed by Faradaic reactions for these two electrolytes. Whereas no redox peaks were observed on cyclic voltammetry curves of CH_3COONa and NH_4Cl electrolytes for all scan rates which indicates that the supercapacitive behaviour for these electrolytes is purely based on the electrostatic mechanism and charge-discharge process of active materials occurs at a pseudo-constant rate over a whole potential window [9].

From all the figures, it is also proved that for higher scan rate potential window as well as current associated with the CV curve increases with increase in scan rate. Which indicates that voltammetric current is directly proportional to the scan rates of CV and this is an indication of good supercapacitive behaviour.

Table 1 shows the specific capacitance values with various electrolytes for different scan rates. For KOH electrolyte, which is having high molar conductivity as compared to other electrolytes [9] highest specific capacitance 675 F/g is observed for that. Whereas KCl exhibited pseudocapacitance nature according to cyclic voltammogram, specific capacitance obtained is 172 F/g at 10 mV/s scan rate. Whereas low specific capacitance of 80 F/g and 56 F/g were obtained for CH_3COONa and NH_4Cl electrolytes respectively as they have low molar conductivity.

Cyclic stability: Retaining of specific capacitance for long redox cycles at higher scan rate operation condition is essential for practical applicability of a supercapacitor. Figure 4 shows the CV curves with KHO, KCl, NH_4Cl and CH_3COONa electrolytes for 1st and 1000th cycles

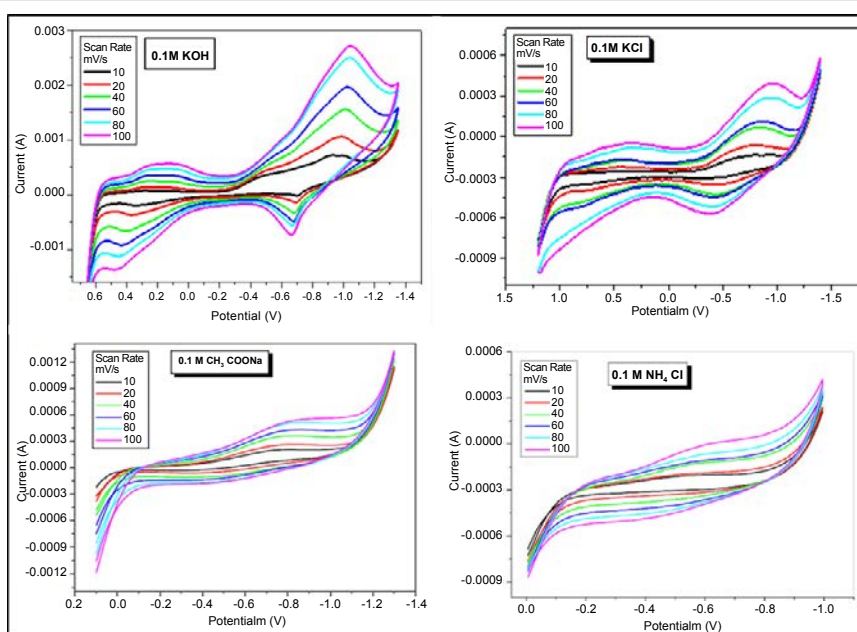


Figure 3: Cyclic voltammogram curves of supercapacitor for different aqueous electrolytes.

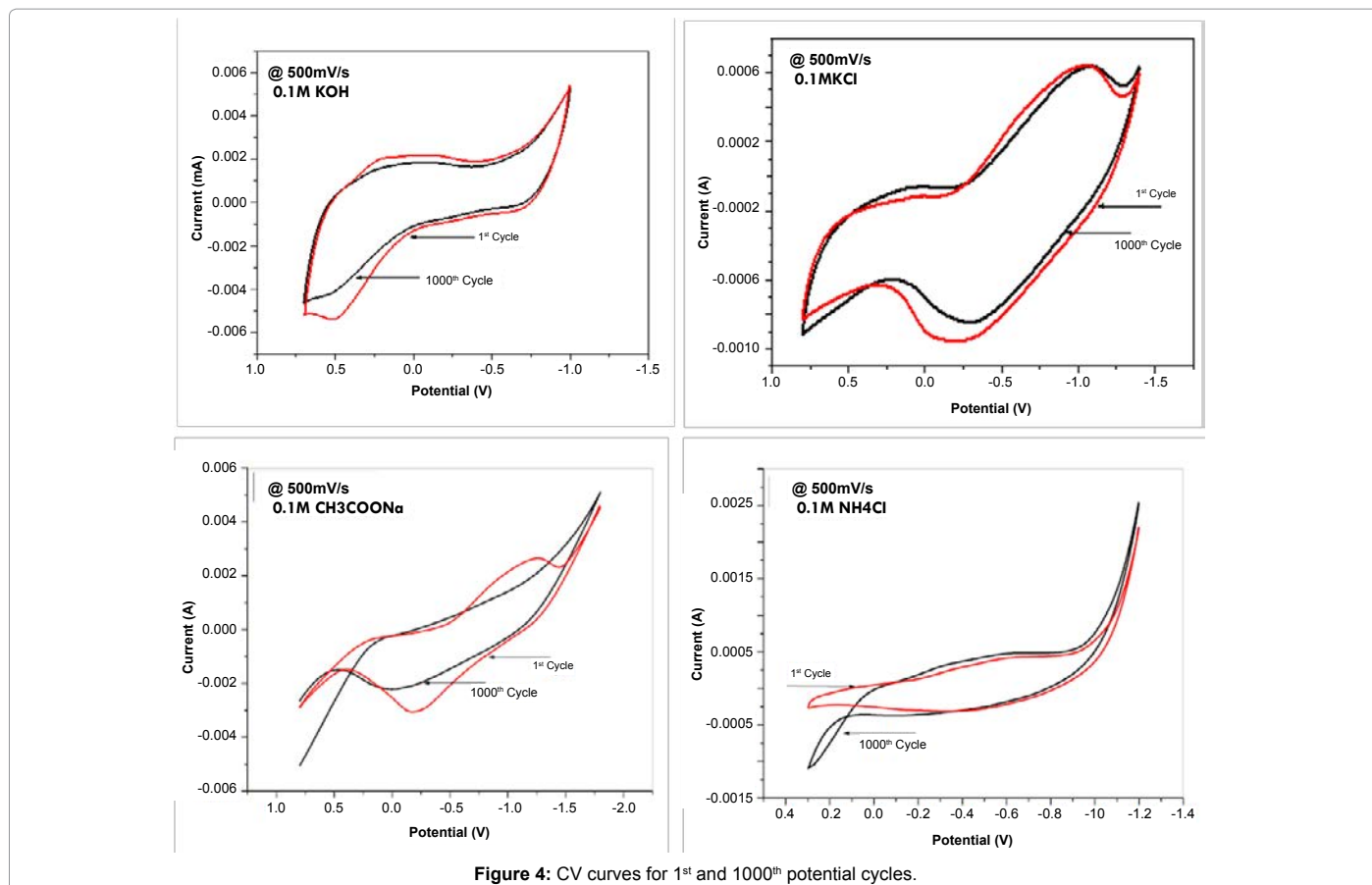


Figure 4: CV curves for 1st and 1000th potential cycles.

Scan Rate (mV/s)	Specific Capacitance (F/g)			
	KOH	KCl	CH ₃ COONa	NH ₄ Cl
10	675	172	80	56
20	620	163	76	42
40	524	144	65	35
60	465	130	54	30
80	424	124	50	28
100	393	108	43	26

Table 1: Specific Capacitance values for various electrolytes.

Electrolytes	Stability (%)
KOH	88.9
KCl	90.01
CH ₃ COONa	64.06
NH ₄ Cl	60.24

Table 2: Percentage stability of with different electrolytes.

at the scan rate of 500 mV/s. All Cyclic voltammograms for 1st and 1000th potential cycles showed no major changes between CV's and the total charge enclosed by both the curves are probably similar to each other, illustrating the stable nature of electrode in the energy storage application.

Table 2 shows the percentage stability of supercapacitor for different electrolytes. It can be found that electrode can withstand about 1000 cycles without a significant decrease in the capacity, with various electrolytes, illustrating the stable nature in energy storage application. The specific capacitance values are decreased in small amount with the number of cycles due to the loss of active material [14]. Among

the electrolytes KOH and KCl attained good cyclic stability of 88.90 and 90.01 respectively over 1000 cycles. It indicates that the material behave reversibly as an excellent capacitor material for large number of potential cycles.

Electrochemical impedance analysis: Electrochemical Impedance Analysis was carried out to know the internal resistive parameters and capacitive behaviour of the supercapacitor at different operating open circuit potentials in KOH, KCl, CH₃COONa and NH₄Cl electrolytes each of 0.1 M concentration. Figure 5 shows the Nyquist plot of Z'' vs. Z' obtained by simulation using ZsimpWin software. The electrodes were excited with 5 mV AC signal and impedance was measured at open circuit potential in the frequency range from 1 Hz to 0.1 MHz [15].

The EIS figures show the small semicircle (first segment), Warburg diffusion line (second segment) and capacitive line (third segment). The beginning of the semicircle line (left-intercept of Z'' at the Z' axis) represents the resistance (R_s) of the electrolyte in contact with the current collector and electrode. The termination of the semicircle line (right-intercept of Z'' at the Z' axis) represents the internal resistance (R_p) of the electrode. The diameter of the semicircle (R_p-R_s) is equal to the ESR value. The second segment (straight line with a slope of approximately 45°) in the middle frequency region represents the combination of resistive and capacitive behaviours of the ions penetrating into the electrode pores. The length, slope and position of this segment appear to be different with each electrolyte. The third segment (straight lines sharply increasing at the low-frequency region) represents the dominance of capacitive behaviour from the formation of ionic and electronic charges of the electric double layer system at the

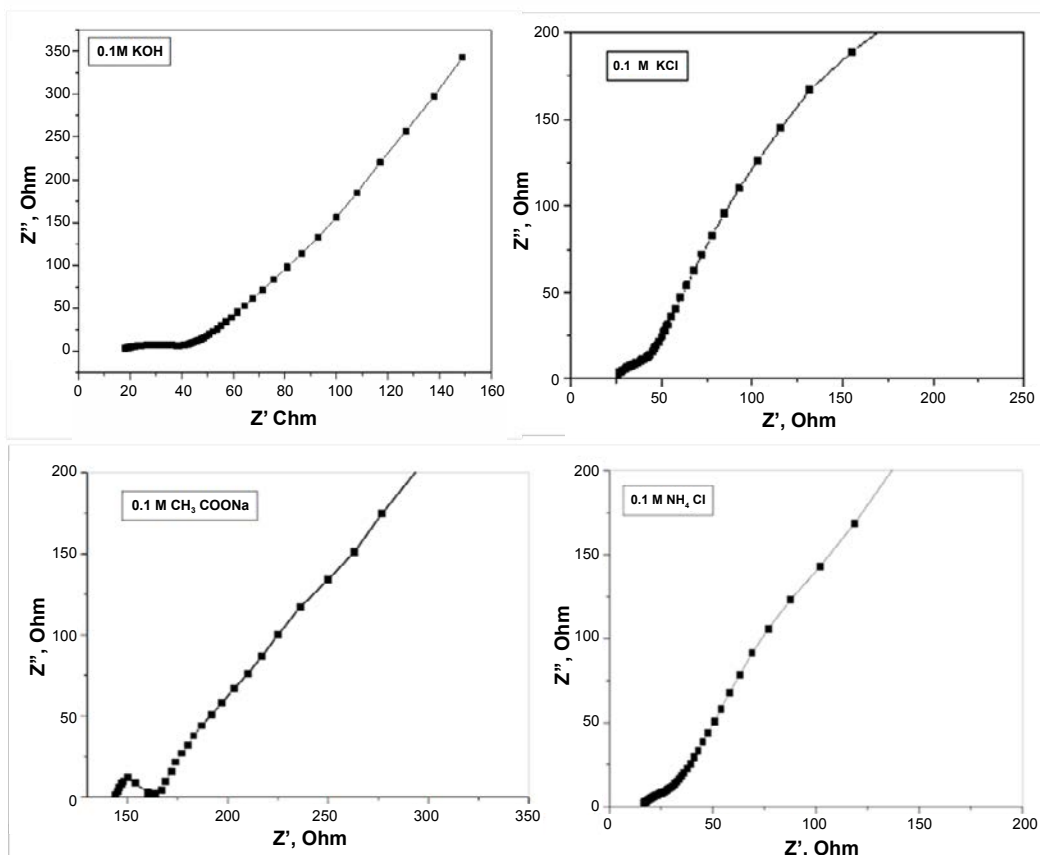


Figure 5: Nyquist plots for various electrolytes.

Electrolytes	R_s (Ω)	R_p (Ω)	ESR (Ω)	f_k (Hz)	R_k (Ω)
KOH	12	20	8	97	24.5
KCl	26.7	40.6	13.3	57.4	27.6
CH ₃ COONa	143	160	17	31.6	174
NH ₄ Cl	16.2	40	23.8	31.6	25.9

Table 3: Values of R_s , R_p , ESR, f_k and R_k for different electrolytes.

micropore surfaces at this frequency, the ions can more easily diffuse into the micropores. The initiation point of this third segment line corresponds to the knee frequency (f_k), and its corresponding resistance (R_k) is given by Z'_k [16-20]. The values of f_k and R_k are given in Table 3.

The values of R_s , R_p , ESR, f_k and R_k for all the electrolytes determined from the Figure 3 are listed in Table 3. The magnitude of the ESR value is found to be maximum for NH₄Cl electrolyte. And minimum value of ESR is obtained for KOH electrolyte 8.0 Ω exhibiting highest specific capacitance.

Conclusion

Among the various aqueous electrolytes studied, KOH, KCl, CH₃COONa and NH₄Cl studied KOH revealed good electrochemical characteristics. For KOH electrolyte, the cell revealed specific capacitance of 675 Fg⁻¹. The specific capacitance values are decreased after 1000 cycles, but showed good reversible activity. For KCl electrolyte cyclic stability was 90.01% and for KOH it was 88.90. The magnitude of the ESR value is found to be minimal for KOH i.e., 8 Ω . From overall electrochemical analysis it was found that supercapacitor

with 1% Mn doped cobalt oxide thin film electrode showed good electrochemical behaviour with KOH electrolyte.

References

- Conway BE (2013) Electrochemical supercapacitors: scientific fundamentals and technological applications. Springer Science and Business Media.
- Lota K, Sierczynska A, Acznik I (2013) Effect of aqueous electrolytes on electrochemical capacitor capacitance. *Chemik* 67: 1138-1145.
- Dvořák P (2010) Overview of Non-Aqueous Electrolytes for Supercapacitors. FECC BUT.
- Gao Q (2013) Optimizing carbon/carbon supercapacitors in aqueous and organic electrolytes (Doctoral dissertation, Université d'Orléans).
- Hu CC, Chang KH, Wang CC (2007) Two-step hydrothermal synthesis of Ru-Sn oxide composites for electrochemical supercapacitors. *Electrochimica acta* 52: 4411-4418.
- Chang KH, Hu CC (2006) Hydrothermal synthesis of binary Ru-Ti oxides with excellent performances for supercapacitors. *Electrochimica Acta* 52: 1749-1757.
- Hu CC, Guo HY, Chang KH, Huang CC (2009) Anodic composite deposition of RuO₂·xH₂O-TiO₂ for electrochemical supercapacitors. *Electrochemistry Communications* 11: 1631-1634.

8. Hu CC, Yang YL, Lee TC (2010) Microwave-Assisted Hydrothermal Synthesis of RuO₂·xH₂O-TiO₂ Nanocomposites for High Power Supercapacitors. *Electrochemical and Solid-State Letters*, 13: A173-A176.
9. Joshi PS, Jogade SM, Gothe SD, Sutrave DS (2017) Cyclic Voltammetric Analysis of Ruthenium Oxide Thin Film Electrodes: Effect of Aqueous Electrolytes. *Asian Journal of Chemistry* 29: 203.
10. Wang G, Zhang L, Zhang J (2012) A review of electrode materials for electrochemical supercapacitors. *Chemical Society Reviews* 41: 797-828.
11. Toupin M, Bélanger D, Hill IR, Quinn D (2005) Performance of experimental carbon blacks in aqueous supercapacitors. *Journal of power sources* 140: 203-210.
12. Jogade SM, Sutrave DS, Patil VB (2016) Structural and Morphological Properties of Mn-Doped Co₃O₄ Thin Film Deposited by Spin Coat Method 6: 41-46.
13. Jagdale AD (2012) Dissertation Thesis: Supercapacitor based on Electrosynthesized Cobalt oxide and Nickel Oxide Thin Films. Shivaji University, Kolhapur, Maharashtra, India.
14. Zeng H, Tang F, Lim M (2010) *J of Power Sources*, 195.
15. Sarac AS, Ates M, Kilic B (2008) Electrochemical impedance spectroscopic study of polyaniline on platinum, glassy carbon and carbon fiber microelectrodes. *Int J Electrochem Sci* 3: 777-786.
16. Farma R, Deraman M, Awitdrus IA, Talib R, Omar JG, et al. (2013) *Int J Electrochem Sci* 8: 257-273
17. Chen WC, Wen TC, Teng H (2003) Polyaniline-deposited porous carbon electrode for supercapacitor. *Electrochimica Acta* 48: 641-649.
18. Rafik F, Gualous H, Gallay R, Crausaz A, Berthon A (2007) Frequency, thermal and voltage supercapacitor characterization and modeling. *Journal of power sources* 165: 928-934.
19. Nian YR, Teng H (2003) Influence of surface oxides on the impedance behavior of carbon-based electrochemical capacitors. *Journal of Electroanalytical Chemistry* 540: 119-127.
20. Gamby J, Taberna PL, Simon P, Fauvarque JF, Chesneau M (2001) Studies and characterisations of various activated carbons used for carbon/carbon supercapacitors. *Journal of power sources* 101: 109-116.